

This is the peer reviewed version of the following article: Zhang, J., Liu, X., & Senousi, A. M. (2021). A multilayer mobility network approach to inferring urban structures using shared mobility and taxi data. *Transactions in GIS*, 25(6), 2840-2865, which has been published in final form at <https://doi.org/10.1111/tgis.12817>. This article may be used for non-commercial purposes in accordance with Wiley Terms and Conditions for Use of Self-Archived Versions. This article may not be enhanced, enriched or otherwise transformed into a derivative work, without express permission from Wiley or by statutory rights under applicable legislation. Copyright notices must not be removed, obscured or modified. The article must be linked to Wiley's version of record on Wiley Online Library and any embedding, framing or otherwise making available the article or pages thereof by third parties from platforms, services and websites other than Wiley Online Library must be prohibited.

# 1     **A Multilayer Mobility Network Approach to Inferring Urban Structures Using** 2     **Shared Mobility and Taxi Data**

3  
4

## 5     **Abstract**

6     Developing data-driven approaches to understanding urban structures is important for  
7     urban planning. However, it is still challenging to combine different transport datasets  
8     into a unified framework and reveal the dynamics of urban structures with the  
9     emergence of shared mobility. In this study, we propose two empirical multilayer  
10    networks to infer and profile urban structures. First, a temporal network is constructed  
11    using traditional taxi data over years to reveal the urban structures. Second, a  
12    multimodal network is constructed using shared mobility and traditional taxi data over  
13    a year to reveal the urban structures. The proposed networks are tested in New York  
14    City using a large volume of shared bike, shared vehicle, and traditional taxi data. The  
15    multilayer network centralities and community detection enable us to profile the  
16    characteristics of the urban flows and urban structure. The analytical results allow us to  
17    acquire a better understanding of urban structures from a multilayer perspective and  
18    also provide a geocomputation framework that is useful for urban and geographic  
19    researchers.

20

21    **Keywords:** Urban structure, shared mobility, multimodal transport, multilayer  
22    network.

23

## 24    **1. Introduction**

25    Urban structure refers to the spatial arrangement of land use in urban areas. It has been  
26    a subject of interest for geographers and urban planners to explain the urban structure  
27    based on social demographics or environmental settings (Rodrigue et al, 2009). In  
28    recent decades, the knowledge about urban structure has extended due to massive  
29    individual-level and high-frequency mobility data (Zhong et al., 2014; Sarkar et al.,  
30    2017; Zhang et al., 2018; Yildirimoglu & Kim, 2018). Based on the new datasets and  
31    analytical approaches, one can observe and infer urban structures that are formed by  
32    diverse types of travel behavior reflected by travel flows, namely orientation-  
33    destination (OD) data. Similar to spatial borders formed by physical configurations (e.g.,  
34    rivers and mountains), the compound effect of facilities and travel purposes  
35    differentiates one zone from another, which works as an underlying structure (Jiang &  
36    Yao, 2010). Hence, mobility data are important to capture the travel behavior that  
37    emerged due to the underlying urban structure, and vice versa.

38    Relations and interactions between places play a critical role in the process of  
39    inferring the urban structure (Rodrigue et al, 2009). To capture such interactions,  
40    transport flows and mobility patterns have been mostly exploited from a network  
41    perspective (Barthélemy, 2011; Zhong et al., 2014; Zhang et al., 2018). In the context  
42    of network theory, the spatial structure of cities is inferred by modeling travel behavior  
43    using graphs. A graph that represents places as nodes and travel flows between nodes  
44    as edges can be partitioned into subgraphs, each of which is a collection of similar nodes  
45    (e.g., similar places in urban context). In practice, the projection from the network  
46    structure to the urban structure has been empirically tested in large-scale  
47    communication networks (Ratti et al., 2010) and mobility networks (Zhong et al., 2014;  
48    Zhang et al., 2018). However, it should be noted that there are two major challenges  
49    that remain in existing works. First, different mobility data may unveil the urban  
50    structure from different interaction perspectives, but single source data are insufficient

51 overall for evaluating the urban structure. Second, those studies that compared travel  
52 patterns of multiple transport data treat and analyze each type of transport flow  
53 separately. Advancing the approach to better integrate and compare multiple data  
54 sources for urban structure inference is necessary to tackle the increasing complexity  
55 of travel behavior. The travel flows of different transport modes at different times are  
56 the multiple facets/layers existing in the same urban space, which will contribute to a  
57 more comprehensive understanding of urban structures.

58 In this study, we adopt the advanced definition and methods of network theory,  
59 i.e., multilayer network analysis, to represent multidimensional travel flows and to  
60 understand multilayer urban structures. A multimodal network model consisting of both  
61 shared mobility and traditional taxi data in a year and a temporal network model  
62 consisting of taxi data over six years are proposed and analyzed to explore the urban  
63 structures. Instead of layer-by-layer analysis, we integrate multiple datasets in a  
64 multilayer network, and the node centralities and community detection in this context  
65 make it possible to compare the feature differences among urban locations (i.e., nodes  
66 in network). The novelty of the approach is demonstrated in a case study in New York  
67 City, which aims to make new contributions to the following research questions: (1)  
68 what are the travel patterns in the multilayer mobility network consisting of shared  
69 mobility for traditional taxis, (2) what urban structures are inferred in terms of  
70 multilayer place importance, and (3) what urban structures are inferred and varying in  
71 the different layers (i.e., transport modes and years) of a multilayer network? The  
72 approach used in this study is a new adoption of network theory in the field of urban  
73 structure analysis considering shared mobility, which can be further used as a  
74 geocomputation method when studying other urban issues.

75 The remainder of this work is structured as follows. Section 2 presents the related  
76 work to justify the feasibility of analyzing urban structures based on mobility networks  
77 and summarizes existing knowledge on shared mobility and the advantages of  
78 multilayer network analysis. Section 3 briefly introduces the study area and multisource  
79 transport data. Section 4 presents the methodology of defining the empirical multilayer  
80 network models for the proposed questions and explains the techniques used for  
81 analysis. Section 5 presents the results, and we discuss and conclude the entire study in  
82 Section 6.

83

## 84 **2. Related work**

85 The inference of urban structures based on travel patterns has a long history in the  
86 geography research (Handy, 1996). However, the methods and insights are still limited  
87 due to the lack of large-scale location data. In recent decades, ubiquitous GPS-enabled  
88 sensing technologies have made positioning data increasingly available at the  
89 individual level. Such an empirical dataset makes it possible to observe and analyze  
90 human mobility and the underlying urban structure at a finer resolution. Abundant work  
91 has utilized positioning data to investigate travel behavior using spatial-temporal  
92 perspectives (Tao et al., 2014; Luo et al., 2017; Li et al., 2019) and transport mode  
93 choices (Paulssen et al., 2014; Klinger & Lanzendorf, 2016; Li et al., 2019). Several  
94 early studies adopted network analysis to understand the urban structure from the  
95 spatial interactions extracted from mobility data (Zhong et al., 2014; Sarkar et al., 2017;  
96 Zhang et al., 2018). Similarly, researchers in the time geography field have argued that  
97 mobility-related big data make it more feasible and effective to link travel patterns and  
98 urban structures (Chen et al., 2016). Although these studies reveal urban structure  
99 projects based on the properties or topology of mobility networks, the multidimensional  
100 complex interactions cannot be effectively characterized from the analysis of monoplex

101 (i.e., single-layer) network. In addition, network communities detected in single-layer  
102 networks are not directly comparable, making it difficult to analyze the variation of  
103 interaction patterns and the associated urban structure.

104 Mobility-related big data of traditional transportation (e.g., travel records of buses  
105 and taxis) have been widely used to proxy urban flows and reveal urban structures  
106 (Zhong et al., 2014; Zhang et al., 2018). However, limited research has extracted urban  
107 flows and related urban structures using shared mobility data. In particular, the possible  
108 changes in the travel context due to the emergence of the new travel modes should be  
109 quantitatively modeled and analyzed. In recent years, the rise of shared mobility  
110 services (e.g., shared taxis and shared bikes) has occurred in many cities due to the wide  
111 use of smartphones and seamless information exchange platforms (Cannon & Summers,  
112 2014). These services have been reported as one of the major travel options besides  
113 traditional transportation systems (Cannon & Summers, 2014; Wallsten, 2015). The  
114 automatic collection of shared mobility data has facilitated urban dynamics research in  
115 various topics. Most literatures are dedicated to evaluating the benefits of shared  
116 transportation for traffic conditions (Shmueli et al., 2015; Alexander & González, 2015;  
117 Li et al., 2016) and exploring travel patterns (Qian et al., 2015; Hochmair, 2016; Xu et  
118 al., 2019). The travel patterns of shared taxis significantly differ from the traditional  
119 patterns in supplementing distant commuting while the travel patterns of shared bikes  
120 are highly associated with public transport stations (Shen et al., 2017; Cao et al., 2019).

121 Follow-up studies consider and compare multiple urban flows of traditional and  
122 shared transportation to study travel behavior. The changes are significant in some ways.  
123 For example, shared bikes particularly reduce bus ridership and work more efficiently  
124 in dense areas than traditional taxis (Campbell & Brakewood, 2017; Faghih-Imani et  
125 al., 2017). There is very limited research on shared mobility flows using graph analysis.  
126 Yang et al. (2019) applied graph-based analysis to shared bike mobility data and  
127 quantified the temporal changes in travel structures, providing empirical evidence on  
128 urban metabolism theory. The study shows that network theory is quite important for  
129 understanding urban structures while the lack of considering multiple mobility flows in  
130 the same framework may not be as complex as the real situation. A more comprehensive  
131 framework to handle the complexity of multidimensional mobility data to understand  
132 travel behavior and urban structure is on the agenda.

133 Urban space bears various travel interactions at the same time, which means that  
134 multiple distinct networks exist and interact simultaneously. The fundamental  
135 advantage of network theory is that the network model and metrics effectively represent  
136 the processes and dynamics in real-world cases (e.g., Barabasi, 2005; Newman, 2006).  
137 In the context of cities, Batty (2013) proposed a new paradigm known as “*The new  
138 science of city*” that emphasizes the importance of considering flows among different  
139 entities in urban analytics. However, in nature, real-world systems are composed of  
140 multidimensional interactions (e.g., cooccurrence or interdependent interactions), and  
141 a single-layer network may provide biased conclusions for systems that consist of  
142 subsystems (Battiston et al., 2017). Although city and travel transit are similar to such  
143 complex systems, early studies focused more on single networks due to the limited  
144 development in network science (Ferber et al. 2005; Dimitrov & Ceder 2016). A  
145 multilayer network considers the co-occurrence of multiple relationships into the  
146 topology, which fits the real-world scenario and the topic of this paper better.

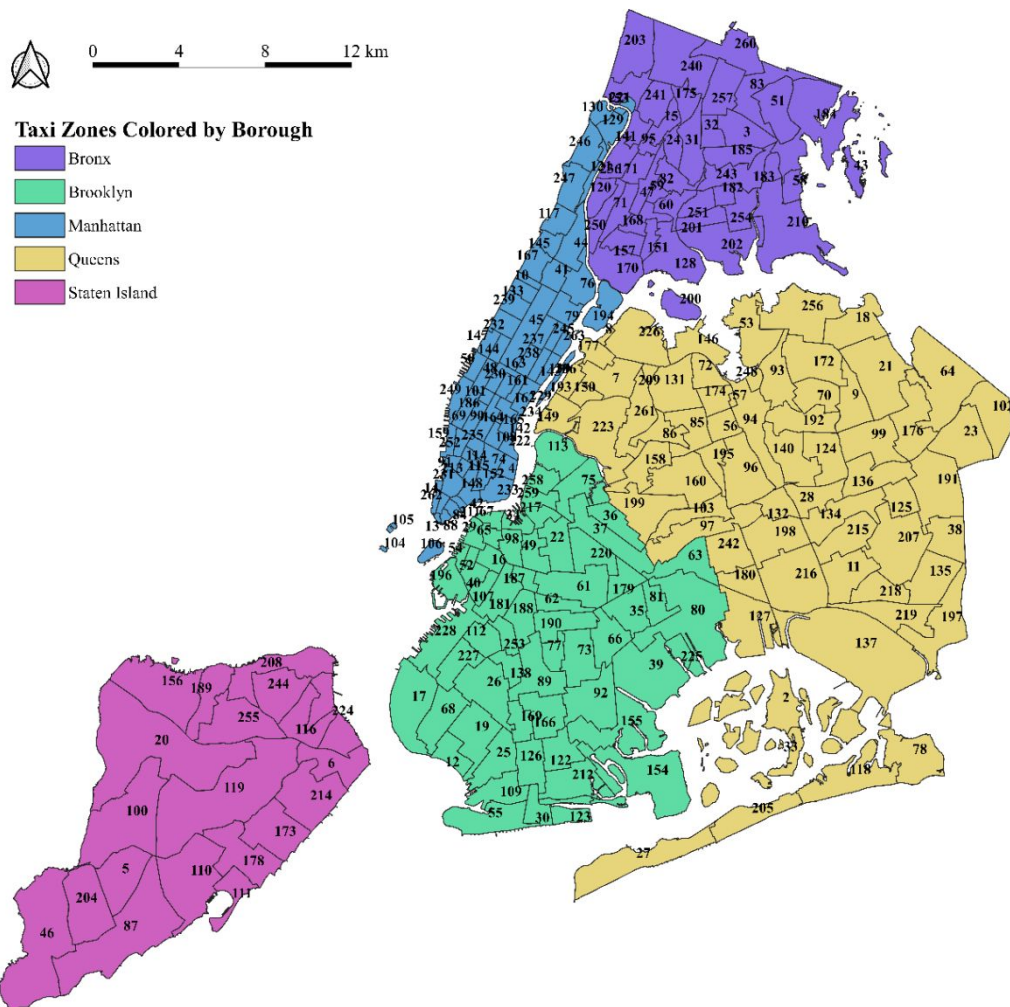
147 Recent developments in multilayer networks have made substantial progress.  
148 Besides extending the network definition by adding ‘layer’ and ‘aspect’, some network  
149 measures (e.g., centralities) are extended to analyze the structure of a multilayer  
150 network. With the new framework and techniques, Parshani et al. (2011) examined the

151 robustness of the two-layer network structure of port and airport networks worldwide.  
152 Halu et al. (2014) model Indian air and train transportation as a multilayer network and  
153 find that the heterogeneity of the two networks enables good navigability performance  
154 of the global network. In recent years, a number of studies have applied multilayer work  
155 in various scenarios such as predicting epidemic transmission (Zhao et al., 2014),  
156 accessibility models (Strano et al., 2015; Aleta et al., 2017), social-physical travel  
157 behavior (Hristova et al., 2014 May; Gao & Tian, 2019), and urban structures  
158 (Yildirimoglu & Kim, 2018). According to the existing literatures, multilayer network  
159 analysis has great potential in modeling human mobility networks while empirical  
160 studies on urban structures are quite limited.

161

### 162 **3. Study area and datasets**

163 New York City (NYC), which has a population of approximately 8.4 million, is one of  
164 the largest megacities in the United States. A total of 264 taxi zones are the spatial unit  
165 in this study (Figure 1). Newark, a taxi zone outside the NYC, is not included in the  
166 following analysis, this paper focuses on the zones within five NYC boroughs. Taxi  
167 zones are the official boundaries for pricing and analyzing taxi trips and therefore are  
168 naturally suitable to analyze shared vehicles. Since the taxi zones are relatively dense  
169 in the Manhattan area, where shared bikes play the same important role as other  
170 transport modes in this region (Faghih-Imani et al., 2017), we argue that the selected  
171 spatial unit is suitable to capture human mobility using shared bikes. Using the same  
172 spatial unit, the taxi zones are used to extract the interzone urban flows of different  
173 layers (e.g., modes and years) and regarded as nodes in the multiplex network, which  
174 will be further discussed in Section 4.



175

176

Figure 1. Study area: Taxi zones in the New York City Boroughs

177

178

179

180

181

182

183

184

185

186

187

188

189

190

191

192

193

194

Several open-data initiatives make it easier to access human mobility and transport datasets. Specifically, three types of trip data are collected from the NYC Taxi and Limousine Commission (TLC)<sup>1</sup>, namely, yellow taxi, green taxi, and for-hired vehicle (FHV) data. As strong competitors to traditional public transport, shared mobility services have become important alternatives for daily travel in cities. Such datasets are able to capture human mobility on a large scale with a fine resolution and better spatial coverage. Yellow taxis are allowed to pick up passengers in any zone while green taxis are mainly allowed to serve outer boroughs (i.e., districts outside Manhattan). Yellow taxis and green taxis are integrated and treated together as traditional transport in this study. FHV data contain the trips made by taking a shared vehicle (e.g., Uber and Lyft). An FHV is distinguished from traditional taxis in that drivers and passengers are freer to choose each other and choose orientation-destination pairs via online platforms. In addition to shared vehicles, shared bikes are another popular mode for commuting in NYC. We collected bike data from the City Bike data portal<sup>2</sup>, which is the largest bike sharing system in the city.

The temporal scheme for data collection and analysis is the monthly snapshot of 6 incremental years to decrease the computational complexity. Specifically, the August data of each year from 2013 to 2018 are collected. We choose these years because the

<sup>1</sup> <https://www1.nyc.gov/site/tlc/about/tlc-trip-record-data.page>

<sup>2</sup> <https://www.citibikenyc.com/system-data>

195 market share of shared mobility services started to increase during the period, which  
 196 may bring changes to the context that was originally dominated by traditional taxis. The  
 197 useful attributes of different types of data, including the pick-up and drop-off time and  
 198 location of each trip, are similar (Tables 1-4).

199 Few data cleaning and preparation steps are conducted when generating mobility  
 200 networks. First, data rows with missing values or values in inconsistent formats are  
 201 deleted. Duplicated data rows are also deleted. Because the format of location  
 202 information in yellow and green taxis is different from 2016 onwards, trip data with  
 203 coordinates are required to be spatially joined to be projected to the taxi zone level.  
 204 This step results in OD trips of different data from zone to zone, and such alignment of  
 205 the spatial units is important because zones will serve as the same set of nodes in the  
 206 multiplex transit network.

207 As this study aims to detect urban structures from the overall multilayer interaction  
 208 patterns, the variation in hours or weeks is not included. Hence, the number of trips in  
 209 each month of the year is aggregated at the individual level for any pair of zones, which  
 210 will determine the interaction strength of the edges in each layer (i.e., intralayer edges).  
 211 We believe that the multimodal data spanning from 2013 to 2018 are sufficient to cover  
 212 different aspects of the interaction patterns for investigating urban structures.

213  
 214

Table 1. Sample of yellow taxi dataset

Before 2016					
<b>pickup_datetime</b>	<b>dropoff_datetime</b>	<b>pickup_longitude</b>	<b>pickup_latitude</b>	<b>dropoff_longitude</b>	<b>dropoff_latitude</b>
2013/8/28 18:03	2013/8/28 18:05	-74.007819	40.724951	-74.006129	40.735067
2013/8/31 0:26	2013/8/31 0:35	-74.00044	40.732387	-74.005396	40.711376
...	...	...	...	...	...
2013/8/29 9:26	2013/8/29 9:29	-73.931406	40.760204	-73.920704	40.756749
From 2016 onwards					
<b>tpep_pickup_datetime</b>	<b>tpep_dropoff_datetime</b>	<b>PULocationID</b>	<b>DOLocationID</b>		
2018/8/1 8:29	2018/8/1 8:35	100	90		
2018/8/1 10:07	2018/8/1 10:17	234	234		
...	...	...	...		
2018/8/1 1:21	2018/8/1 1:23	48	143		

215  
 216  
 217

Table 2. Sample of green taxi dataset

Before 2016					
<b>lpep_pickup_datetime</b>	<b>lpep_dropoff_datetime</b>	<b>Pickup_longitude</b>	<b>Pickup_latitude</b>	<b>Dropoff_longitude</b>	<b>Dropoff_latitude</b>
2013/8/28 6:02	2013/8/28 6:13	-73.92948914	40.75686264	-73.92989349	40.75658035
2013/8/26 16:56	2013/8/26 17:05	-73.95521545	40.8044014	-73.97678375	40.7918396
...	...	...	...	...	...
2013/8/31 18:34	2013/8/31 18:39	-73.94673157	40.83132553	-73.94012451	40.84090805
From 2016 onwards					
<b>lpep_pickup_datetime</b>	<b>lpep_dropoff_datetime</b>	<b>PULocationID</b>	<b>DOLocationID</b>		
2018/8/3 7:34	2018/8/3 7:43	95	28		
2018/8/3 22:13	2018/8/3 22:17	255	255		
...	...	...	...		
2018/8/2 22:32	2018/8/2 22:39	65	106		

218  
 219  
 220

221

Table 3. Sample of shared bike dataset

starttime	stoptime	start station latitude	start station longitude	end station latitude	end station longitude
2018/8/2 12:52	2018/8/2 13:00	40.73705	-73.99009	40.73650	-73.97809
2018/8/1 18:54	2018/8/1 19:03	40.74916	-73.99160	40.76009	-73.99462
...	...	...	...	...	...
2018/8/2 13:08	2018/8/2 13:16	40.69128	-73.94524	40.70317	-73.94064

222

223

224

Table 4. Sample of FHV dataset

Pickup_DateTime	DropOff_datetime	PULocationID	DOLocationID
2018/8/23 23:36	2018/8/24 0:01	255	249
2018/8/1 22:33	2018/8/1 22:42	230	90
...	...	...	...
2018/8/2 11:07	2018/8/2 11:31	50	90

225

226

227

## 4. Methodology

228

229

230

231

232

233

234

235

### 4.1. Yearly change rate

236

237

238

239

240

241

242

243

$$\text{Yearly Change Rate (YCR)} = \left( \left( \frac{E_{Trip}}{B_{Trip}} \right)^{1/Y} - 1 \right) * 100 \quad (1)$$

244

245

246

247

248

249

250

251

### 4.2. Generation of transport multiplex network

252

253

254

255

256

257

258

259

260

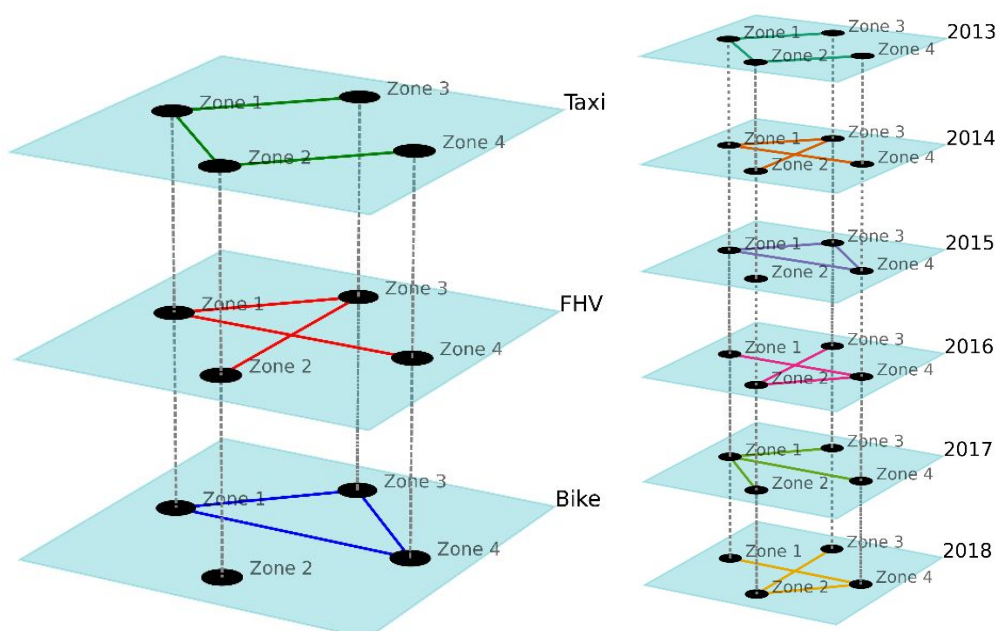
Network analysis has been widely used in analyzing movement data and understanding zone-to-zone behavior (Zhong et al., 2014; Sarkar et al., 2017; Zhang et al., 2018). The recent advancement in network representation and analysis, the multilayer network, has also proven to be effective at including multiple transport entities or relationships in the same framework (Ding et al., 2018; Yildirimoglu & Kim, 2018). Inspired by these works, this study aims to extend the knowledge on multidimensional travel behavior using a multilayer network framework, which is more accurate for describing complex transport systems. The general form of a monoplex (single-layer) network is  $G = (V, E)$ , where  $V$  is the set of nodes and  $E \subseteq V \times V$  is the set of edges connecting each pair

261 of nodes. For the multilayer network, we follow the definition made by Kivelä et al.  
 262 (2014), i.e., a multilayer network  $M = (V_M, E_M, V, L)$ . Edges are allowed to exist between  
 263 any possible pairs of nodes, i.e.,  $E_M \subseteq V_M \times V_M$ . The links between nodes within a layer  
 264 are called intralayer edges, and the links across layers are called interlayer edges. Layers  
 265 of  $d$  aspects are represented by  $L$ , where  $L = \{L_1, L_2, \dots, L_d\}$ . That is, for each aspect,  
 266 there can be multiple layers. For each layer, there are nodes belonging to the same set  
 267  $V$ . For example, an aspect of layers can represent multiple shared mobility modes while  
 268 at the same time another aspect of layers represents multiple public transport modes.

269 In this paper, the multilayer network inferred from empirical transport data is  
 270 known as a multiplex network (Nicosia et al., 2013). The aspect equals 1 in this work,  
 271 which means that networks integrated in the same framework belong to the same type  
 272 (i.e., same year or same mode). Both the orientation-destination direction and trip  
 273 volume are considered in the multiplex network model and in the following analysis.  
 274 In short, direction is considered in multiplex PageRank and modularity, and the number  
 275 of trips among locations determines the intralayer link weights. For the interlayer links,  
 276 we use categorical coupling, which represents the adjacency of a node to itself in other  
 277 layers, to connect layers (Mucha & Porter, 2010; Kivelä et al., 2014). The most common  
 278 weight of the interlayer for the multiplex network is used, and the weight is set to 1  
 279 (Kivelä et al., 2014).

280 A multiplex network is a subset of the general multilayer network, and it has been  
 281 used to study multisource transport data in several literatures (Cardillo et al., 2013;  
 282 Yildirimoglu & Kim, 2018). Compared to the generalized definition of a multilayer  
 283 network, a multiplex network reduces to one aspect, i.e.,  $L = \{L_1\}$ . In the network  
 284 sequence  $\{(V_\alpha, E_\alpha)\}_{\alpha=1}^{\beta}$ , nodes set in different layers are usually the same, i.e.,  $V_\alpha$   
 285  $= V_\beta$  for all  $\alpha$  and  $\beta$ . It is known as an edge-colored graph because it contains the same  
 286 set of nodes but different sets of intralayer edges in each layer (Kivelä et al., 2014).  
 287 Multimodal transport modes and temporal slices can be effectively represented by  
 288 multiplex networks. In general, the following generated networks are directed and  
 289 weighted by the travel flows between zones. Different layers share the same set of nodes  
 290 (i.e., NYC taxi zones) while intralayer links represent different types of human mobility  
 291 interactions between locations.

292



293

294 (a) (b)  
 295 Figure 2. Thematic representation of the multiplex networks in this study: (a)  
 296 Multimodal; (b) Temporal. Note that each layer is a directed graph determined by the  
 297 OD direction, and intralayer links are weighted by the OD volume. The common  
 298 interlayer link weights equal 1 in this study. The multiplex network can effectively  
 299 integrate the occurrence of multi-flows among the same set of locations for analysis.

300 To investigate the impact of on-demand shared transportation, the first multiplex  
 301 network is constructed based on multimodal transit:  $M_{Mode} = (V_m, E_m, L_m)$ , where  $L_m =$   
 302  $\{Taxi, FHV, Bike\}$  and  $E_m \subseteq V_m \times V_m$ . Time is fixed in 2018, and different modes (i.e.,  
 303 taxis, bikes, and FHVs) are regarded as layers. The transit interactions among the same  
 304 set of zones are therefore considered together in the same framework (Figure 2a). Based  
 305 on  $M_{Mode}$ , the experiment focuses on revealing different travel behaviors related to both  
 306 traditional transport (i.e., taxis) and newly emerged modes (i.e., FHVs and shared bikes).  
 307 In contrast, the second generated multiplex network only involves traditional transport  
 308 and taxis but focuses on the possible change in travel behavior over time:  $M_{Time} = (V_t,$   
 309  $E_t, L_t)$ , where  $L_t = \{2013, 2014, \dots, 2018\}$ , and  $E_t \subseteq V_t \times V_t$ . From 2013 to 2018, the taxi  
 310 transit network in each year serves as a layer (Figure 2b). In this period, the context of  
 311 NYC transport gradually changed due to the emergence of shared bikes and shared  
 312 vehicles. As the context changes, the temporal multiplex network of taxis is useful to  
 313 observe whether there is a longitudinal change in travel behavior.

314

### 315 4.3. Centrality metrics

316 Centrality metrics have been widely used to evaluate the importance of nodes.  
 317 Centrality can be regarded as a basic characteristic of a network structure as it indicates  
 318 the levels of heterogeneity of node properties. In a human mobility network, nodes with  
 319 higher centrality may indicate a transportation hub that bears more daily transit and  
 320 activities, which also help to describe the urban structure. In this paper, the degree  
 321 centrality and PageRank centrality are calculated. The degree centrality is the basic  
 322 metric, and PageRank has been used in transport and urban networks to measure the  
 323 attractiveness of a location (Ding et al., 2009; Agryzkov et al., 2016; Jia et al., 2019).  
 324 Although PageRank centrality can be calculated in various domains such as informatics  
 325 (Page et al., 1999), biology (Yu et al., 2017), and human mobility and transport studies  
 326 (Wen, 2015; Xu et al., 2017; Zhou & Qiu, 2018), the network context is still a single  
 327 layer. The extension of centrality measures from monoplex networks to multiplex  
 328 networks is still in its infancy (Battiston et al., 2014; Halu et al., 2013). This study  
 329 depends on the implementation of multiplex centrality measures of MuxViz (De  
 330 Domenico et al., 2015a), specifically multilayer degree centrality (De Domenico et al.,  
 331 2013) and multiplex PageRank centrality (De Domenico et al., 2015b).

332 PageRank is one of most popular algorithms to rank node importance in graphs  
 333 and was proposed by one of the cofounders of Google (Page et al., 1999). PageRank  
 334 measures a node's (e.g., website's) importance based on its outbound links. In the urban  
 335 transport context, this metric reflects how a location attracts outbound interactions from  
 336 other locations, which can be extracted from massive transit data. Therefore, the  
 337 multiplex PageRank extends the capability of this metric in a multilayer context.  
 338 Specifically, in this study, this metric indicates the attractiveness of a location  
 339 considering multimodal flows.

340 For a node  $i$ , it can be calculated as the summation of degree  $k_i^\alpha$  of each layer,  
 341 which is only suitable for a multilayer network without interlayer links. In this paper,  
 342 interlayer links are assumed to exist, that is, the zones on each layer are connected to

343 their counterparts on other layers. Therefore, another improved definition of degree  
344 centrality considering the presence of interlayer links is used in our work:

$$345 \quad k_i = M_{j\beta}^{i\alpha} U_{\alpha}^{\beta} u^j \quad (2)$$

347 where  $k_i$  is the aggregated multilayer degree centrality of node  $i$ ,  $M_{j\beta}^{i\alpha}$  is the  
348 adjacency matrix containing the relationship between node  $i$  on layer  $\alpha$  and node  $j$  on  
349 layer  $\beta$ ,  $L$  is the total number of layers,  $N$  is the total number of unique nodes,  $u^j$  is a  
350 first-order tensor in which all elements equal 1, and  $U_{\alpha}^{\beta} = u_{\alpha} u^{\beta}$  is a second-order tensor  
351 in which all elements equal 1.  
352

353  
354 Early work on generalizing the PageRank centrality to a multilayer network was  
355 performed by Halu et al. (2013). However, their metric is mainly feasible for a two-  
356 layer empirical network due to the complex layer dependence. Here, we rely on the  
357 multiplex PageRank proposed by (De Domenico et al., 2015b). The key idea of  
358 PageRank is to explore the network using the random walk equation, which produces a  
359 transition matrix that defines ‘walk behavior’. In a multiplex network, the PageRank  
360 centrality of node  $i$  is defined as:

$$361 \quad \omega_i = \Omega_{i\alpha} u^{\alpha} = \sum_{\alpha=1}^L \Omega_{i\alpha} \quad (3)$$

363 where  $\omega_i$  is the aggregated PageRank centrality of node  $i$ , and  $\Omega_{i\alpha}$  is the  
364 eigenvector of tensor  $R_{j\beta}^{i\alpha}$ .  
365

$$366 \quad R_{j\beta}^{i\alpha} = \tau T_{j\beta}^{i\alpha} + \frac{(1-\tau)}{NL} u_{j\beta}^{i\alpha} \quad (4)$$

367  
368 where  $\tau$  is the walking rate that is normally set to a constant value (e.g., 0.85),  $T_{j\beta}^{i\alpha}$   
369 is the transition tensor containing the jumping probabilities between pairs of nodes in  
370 any layer,  $N$  is the total number of unique nodes,  $L$  is the total number of layers, and  
371  $u_{j\beta}^{i\alpha}$  is a 4<sup>th</sup>-order tensor in which all elements equal to 1.  
372  
373

374  
375 By adopting these two centrality measures on a multimodal transit network and  
376 temporal taxi transit network, the importance of taxi zones will be evaluated in both  
377 layer-by-layer and aggregated manners.  
378

#### 379 4.4. Community detection in multilayer network

380 In single-layer network analysis, community detection has been proven to be efficient  
381 in characterizing travel preferences from mobility networks (Zhong et al., 2014; Liu et  
382 al., 2015). Given a network, the community detection process partitions and groups  
383 nodes in a manner that maximizes the intergroup distance and minimizes the intragroup  
384 entity distance. In a mobility network generated by urban flows, a community is a  
385 cluster of locations with similar interaction (e.g., in/out flows) patterns. Given a  
386 multimodal network, communities across nodes and layers can be understood as the  
387 variation of interaction patterns across places and different transport modes. The  
388 interpretation of the community in the temporal multiplex network is similar, indicating  
389 variations in interaction patterns across locations and different times. After projecting

390 the network community to geographical space, the interaction-associated urban  
391 structure and its dynamics can be examined.

392 In practice, the most commonly used metric to be maximized is the modularity  
393 (Newman & Girvan, 2004). Despite abundant detection algorithms for monoplex  
394 networks, very few algorithms have been developed in multilayer network frameworks.  
395 Instead of extracting a community layer-by-layer, the multilayer network community  
396 detection algorithm detects the community simultaneously across layers. In this paper,  
397 we utilize the most used multiplex-Infomap algorithm (De Domenico et al., 2015a),  
398 which relies on the refined modularity proposed by Mucha et al (2010).

399

$$400 \quad Q_{multilayer} = \frac{1}{2\mu} \sum_{ijsr} \left[ \left( A_{ijs} - \gamma_s \frac{k_{is}k_{js}}{2m_s} \right) \delta_{sr} + \delta_{ij}\omega \right] \delta(g_{is}, g_{js}) \quad (5)$$

401

402 where  $A_{ijs}$  is the intralayer edge weight between node  $i$  and node  $j$  at layer  $s$ ; the  $k$   
403 of a node is calculated by the sum of the weights of edges attached to this node;  $k_{is}$   
404 represents the total strength (i.e., weighted by trips) for node  $i$  at layer  $s$ ;  $k_{js}$  represents  
405 the total strength of node  $j$  at layer  $s$ ;  $k_{is} = \sum_j A_{ijs}$ ;  $\mu = \frac{1}{2} \sum_{jr} k_{jr}$ ;  $m_s = \frac{1}{2} \sum_{ij} A_{ijs}$ ;  $\delta$   
406 is the Kronecker delta function, which equals 1 if two variables are the same and 0  
407 otherwise;  $g_{is}$  is the community label assigned to node  $i$  in layer  $s$ ;  $\gamma_s$  is a resolution  
408 parameter set to 1 by default; and  $\omega$  is the interlayer coupling weight from 0 to 1, which  
409 equals 1 in this study.

410

411 Most community detection algorithms in networks rely on the concept of  
412 modularity to compress data and find regularities (Grünwald & Grunwald, 2007). The  
413 optimization target is to find the partition structure that minimizes the communication  
414 length. Combining the refined modularity with the classic Infomap algorithm,  
415 multiplex-Infomap can search the community in a multiplex network. In contrast to  
416 single-layer community detection, multiplex-Infomap results in community labels that  
417 are comparable across different layers. For example, zones with the same community  
418 label in different layers (i.e., year or transport mode) indicate that their interaction travel  
419 behaviors are similar, indicating similar urban structures. Therefore, this technique is  
420 efficient in revealing the structure for the first experiment, which investigates the  
421 possible variation between traditional transport (i.e., taxis) and shared transportation  
422 (i.e., bikes and FHV); and for the second experiment, which explores the variation in  
423 traditional taxis from 2013 to 2018.

424

## 425 5. Results

### 426 5.1. Overall trend of multimodal transit in NYC

427 In this section, we examine the basic characteristics of trips by taxis, bikes, and FHVs.  
428 First, the total number of trips in each year of different transport modes is plotted in  
429 Figure 3. A clear trend can be observed in terms of the variation over time. Particularly,  
430 significant variations are found in yellow taxis and FHVs, showing that the number of  
431 trips by yellow taxis has been decreasing since 2013 while that of FHVs is dramatically  
432 increasing. The trip volumes of green taxis and shared bikes are relatively low, and their  
433 variations are weak. Both green taxis and shared bikes are included due to their unique  
434 role in serving specific travel purposes. Green taxis were launched to supplement taxi  
435 services in the outer boroughs, and shared bikes are especially popular in Manhattan  
436 and its surrounding areas. Based on the yearly numbers of trips, a preference shift from  
437 traditional taxis to shared transportation is clearly witnessed.

438

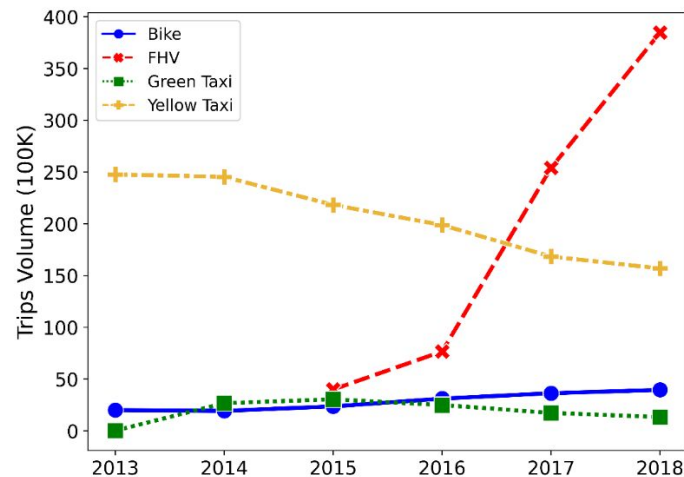


Figure 3. Trip variation of three transport modes over the years

439

440

441

442

443

444

445

446

447

448

449

450

451

452

453

454

455

456

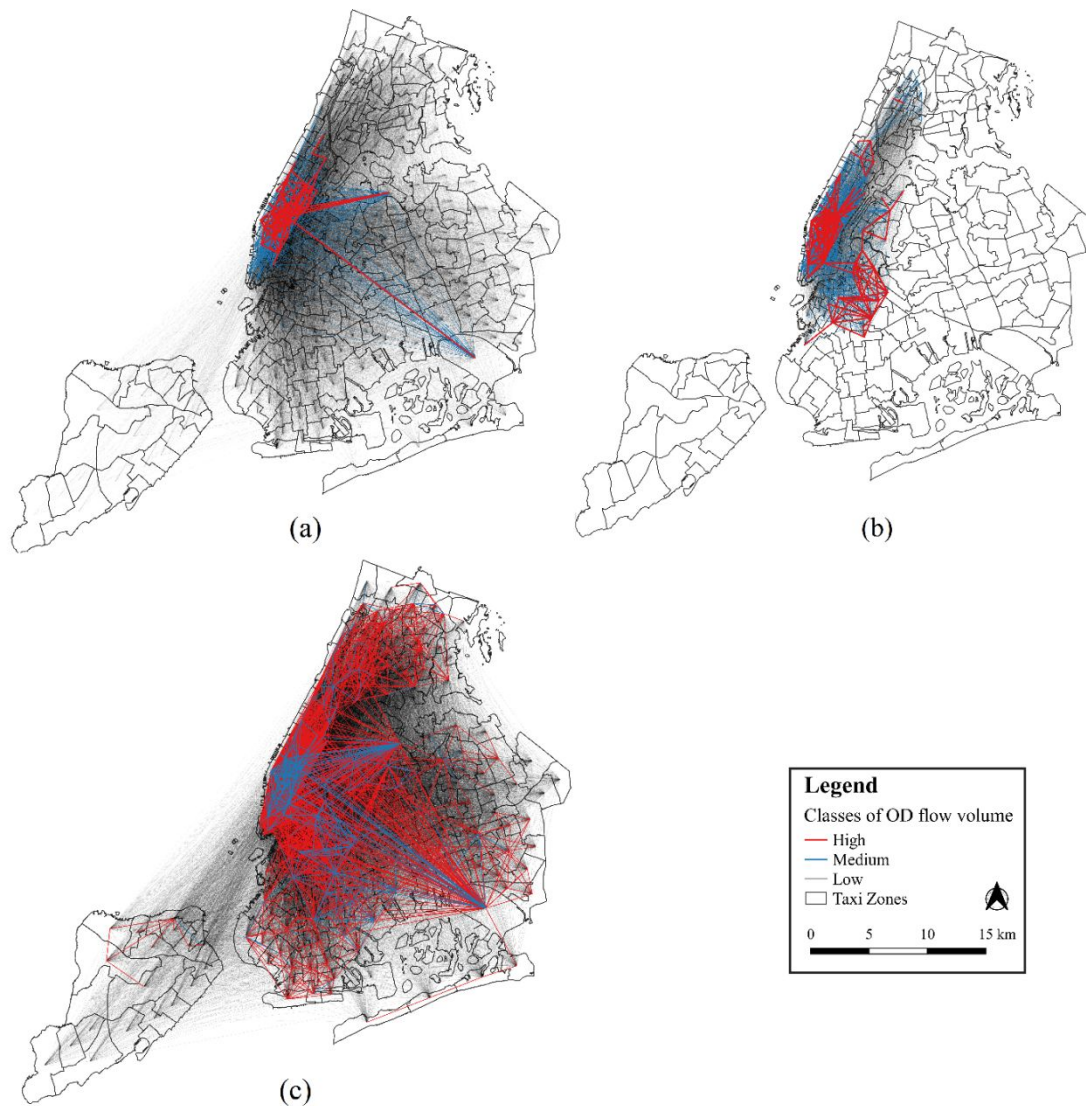
457

458

459

We spatially join the OD trips of all transport modes to the zone level and visualize them on a map (Figure 4), which illustrates how taxis, bikes, and FHVs are differently used in space. Taxi and FHV services cover almost all NYC zones while shared bikes are mainly available in Manhattan and near-Manhattan zones in Brooklyn, Queens, and Bronx. The profound difference between taxis and FHVs is in the distribution of medium (i.e., line in blue) and high volume (i.e., line in red) trips. High trip volumes for taxis are mainly constrained within Manhattan (Figure 4a); in contrast, high trip volumes for FHVs are spread more widely in both Manhattan and the outer zones (Figure 4c). It seems that FHVs not only strengthen the commutes from outer zones to Manhattan but also makes the connections among outer zones stronger.

Taxi drivers may spend less time searching for customers in a more populated dense area (i.e., Manhattan) while the demand-match mechanism in FHVs makes FHVs more flexible to serve more areas. Based on Figure 4, it is obvious that FHVs play a more important role in supplementing the unbalanced supply in distant zones. Shared bikes presents another different spatial pattern, showing that heavy use is mostly in downtown Manhattan and the Brooklyn zones across the river. Additionally, a decent number of bike trips with long travel distances are observed, indicating that shared bikes might be a popular choice for commuting in these areas.



460  
461  
462

Figure 4. Distribution and classification of OD trips: (a) Taxi; (b) Bike; (c) FHV

463

## 5.2. Node centrality in multimodal and temporal mobility networks

464

We first explored the basic law of travel behavior in the multilayer mobility network.

465

Previous researchers observed a heavy-tailed distribution (e.g., power-law or exponential distribution) of displacement and elapsed time (Gonzalez et al., 2008;

466

Liang et al., 2012; Zhao et al., 2015). Using network analysis, Zhong et al. (2014) also

467

reported the heavy-tailed distribution of nodes (i.e., zones) centrality in different modes

468

of the mobility network. However, the node centrality distribution in a multilayer

469

mobility network is limited.

470

471

We calculate two centrality metrics, the multiplex degree and the multiplex PageRank, for both the multimodal network and temporal network. Then, we infer the empirical univariate distribution by using the Python package *distfit*, which fits 89

472

models and ranks the models based on the residual sum of squares (RSS). Overall, node

473

centrality in these two multiplex networks does not follow a power-law or exponential

474

distribution. Instead, the *beta* distribution is identified as the best model for the two

475

centralities in a multimodal network based on the smallest RSS. In multimodal network,

476

most zones (i.e., nodes) have a strong degree centrality and medium PageRank

477

centrality (Figure 5a). The intralayer's centrality (i.e., taxis, bikes, and FHV) and

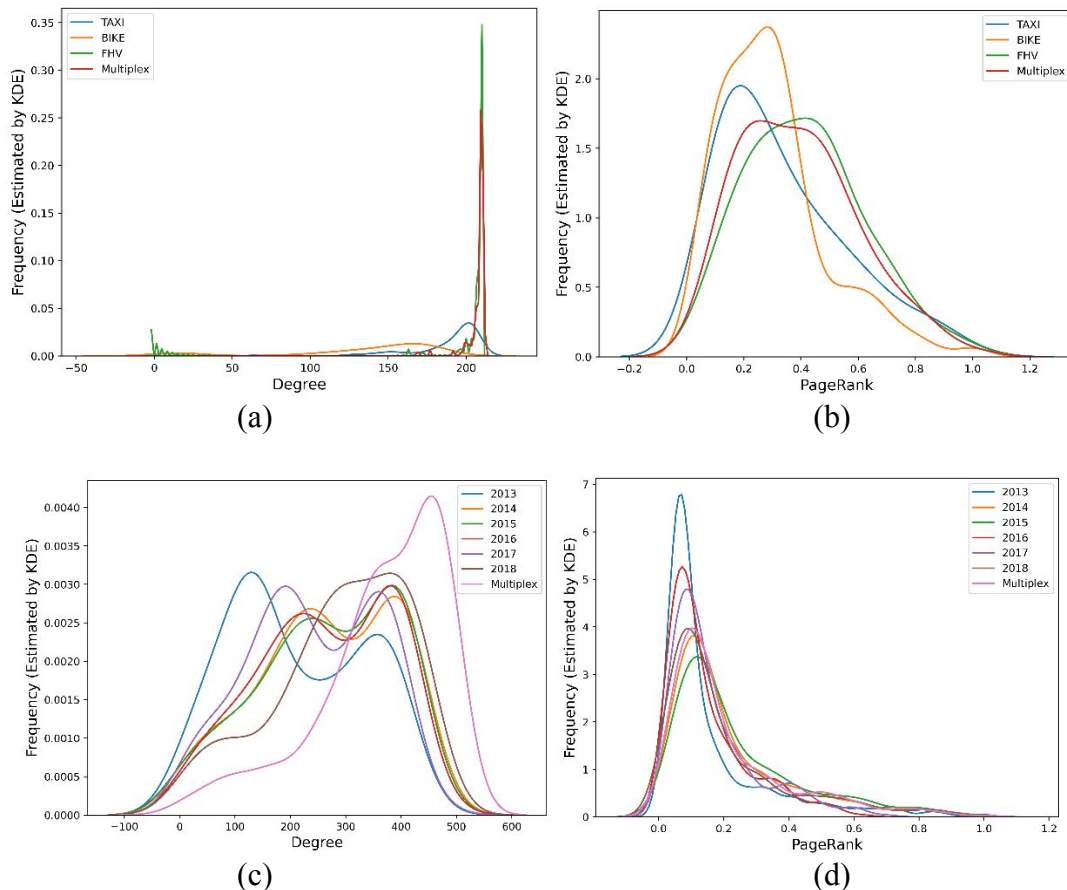
478

aggregated centrality (i.e., multiplex) have relatively similar distributions. A heavy left

479

480

481 tail is found in the degree distribution while a slight right tail is found in the PageRank  
 482 distribution. In temporal network, most zones (i.e., nodes) have a strong degree  
 483 centrality and low PageRank centrality (Figures 5c & 5d). There is significant variance  
 484 among the layers (i.e., 2013 to 2018) in terms of the degree centrality. More zones with  
 485 higher degrees appear chronologically. The PageRank distributions, which all have  
 486 slightly long right tails, are similar among layers.  
 487



491  
 492  
 493 Figure 5. KDE estimated distribution of node centralities: (a) degree in the  
 494 multimodal network; (b) PageRank in the multimodal network; (c) degree in the  
 495 temporal network; and (d) PageRank in the temporal network  
 496

497 Centrality metrics indicate the importance and vibrancy of a location, which may  
 498 reflect the underlying urban structure that breeds such activities (Jia et al., 2019). We  
 499 project the centralities of zones into geographical space (Figure 6), which helps obtain  
 500 a better understanding of the polycentric structure of NYC (Zhong et al., 2014). The  
 501 spatial distribution of multimodal network centralities is different when using the  
 502 degree and PageRank (Figures 6a & 6b). Extreme high degree centralities are mainly  
 503 found in the downtown area of Manhattan while almost all of Manhattan is identified  
 504 as having high PageRank centralities. The possible reason for the heavily left skew of  
 505 the degree is that the Manhattan zones are quite connected when considering multiple  
 506 types of transport modes together (i.e., taxis, bikes, and FHV's). The degree might not  
 507 be the best choice to describe the node importance at such a scale while PageRank is  
 508 able to capture more variance in this well-connected network. Comparatively, the  
 509 spatial distribution of the degree and PageRank centralities of the temporal network  
 510 show similar patterns (Figures 6c & 6d). Manhattan is the most 'important' district in  
 511 terms of the node centralities; moreover, some zones in Brooklyn and Queens show

512 high values. The result of the multiplex centralities in New York City provides evidence  
 513 on the polycentric urban structure reflecting the travel demand.  
 514

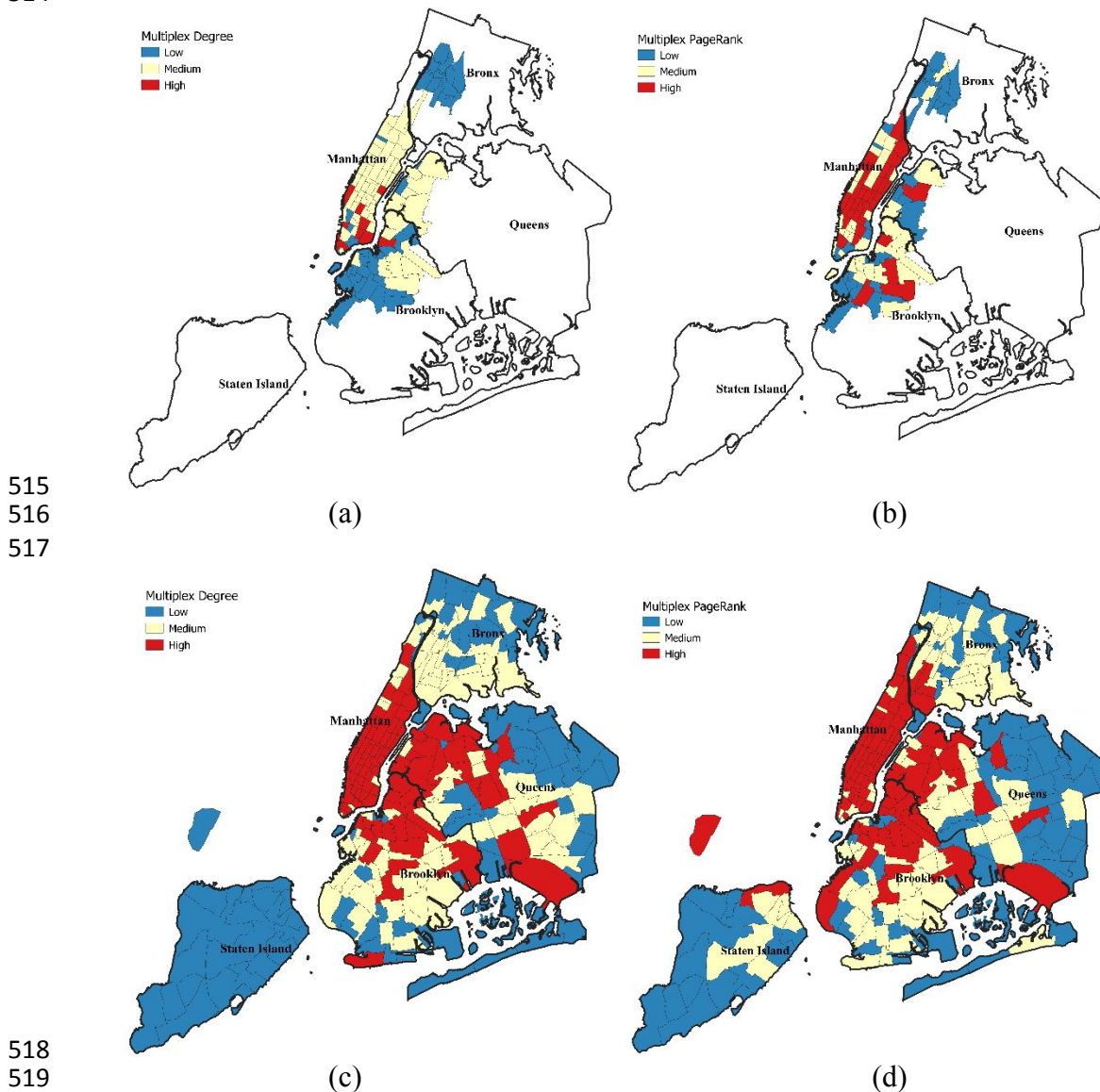
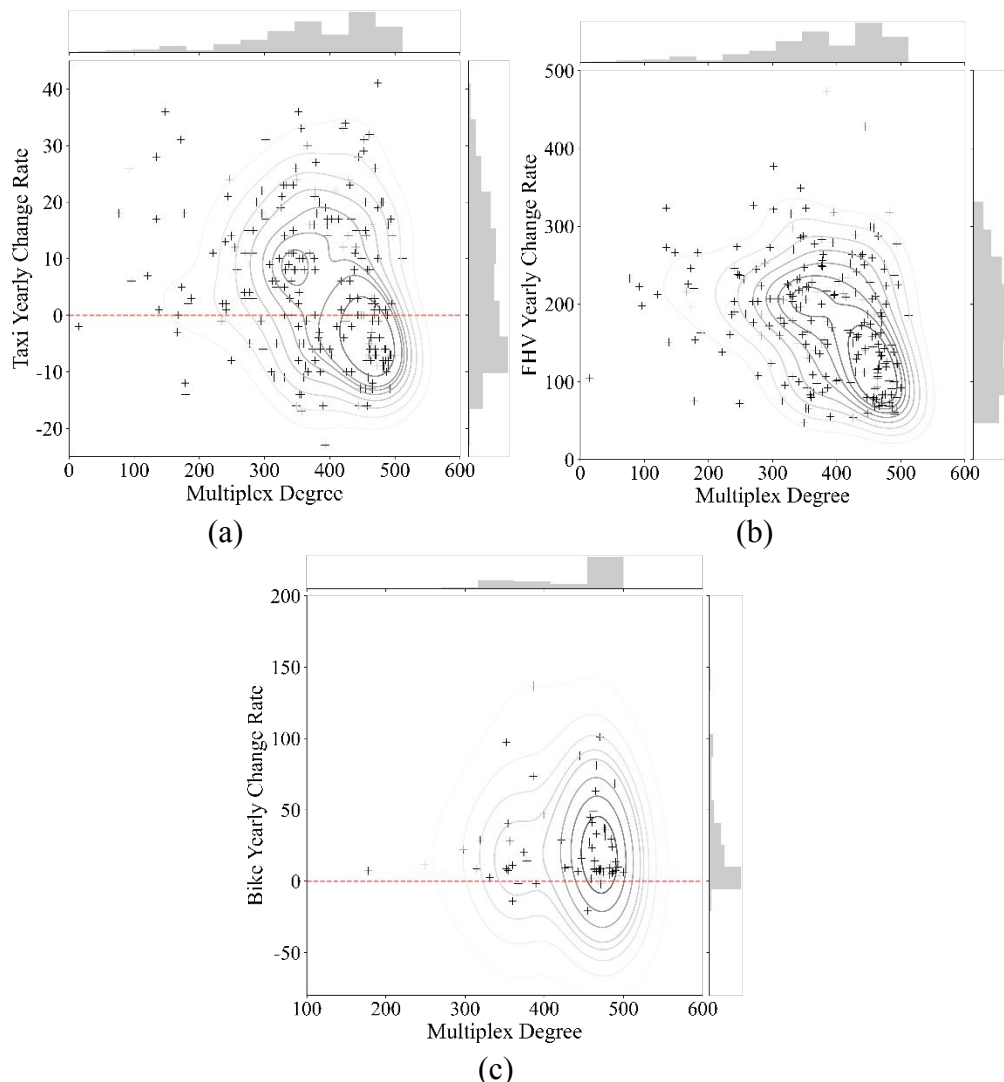


Figure 6. Visualization of the node centralities in geographical space: (a) Degree in the multimodal network; (b) PageRank in the multimodal network; (c) Degree in the temporal network; and (d) PageRank in the temporal network.

The relationship between node (i.e., zone) centrality and trip variation is explored, indicating that the zone importance in the multilayer mobility network is a key indicator correlated to the yearly change rate. Specifically, the node centrality in the temporal network of traditional taxis is selected for comparison for two reasons. First, the multiplex network constructed from taxi data covers the entire city, which provides a more heterogeneous urban context for analyzing the correlation. Second, nodes with high multiplex centrality represent truly important zones for vehicle-based transit because the temporal network takes 6 years of transit patterns in the same framework for evaluation.

In each zone, the yearly change rate is calculated for taxis, FHV's, and bikes, respectively. In Figure 7, each point represents a zone, the X axis represents the multiplex degree, and the Y axis represents the yearly change rate of the specific

536 transport mode. Contour lines are added by the KDE function to indicate the  
 537 concentration patterns, and the dotted horizontal line divides the Y axis into positive or  
 538 negative yearly change rates. Overall, both negative and positive change rates of  
 539 traditional taxis are observed while the change rates of FHVs and shared bikes are  
 540 almost all positive. Similar distribution patterns are observed for taxis and FHVs, which  
 541 indicates that the trip variations of these two vehicle-based transportation systems have  
 542 similar relations to zone importance. Zones with multiplex degrees of approximately  
 543 350 and 450 are dense in Figure 7a and Figure 7b. Yearly change rate of taxi and FHV  
 544 are often lower in higher degree zones (i.e., 450). For traditional taxis, the yearly change  
 545 rate is even negative in such high degree zones, which means that the number of trips  
 546 is decreasing. The number of valid points for shared bikes is less than those for the other  
 547 two modes because the bike data are only available in Manhattan and its near zones  
 548 (Figure 7c). The 450-degree zones play an important role in shared bikes. The node  
 549 centrality of the multiplex mobility network provides a useful indication of location  
 550 importance, which is highly correlated to the variation of different transport modes.  
 551



554  
 555  
 556 Figure 7. Relations between yearly change rate and multiplex node degree: (a) Taxi;  
 557 (b) FHV; (C) Bikes  
 558

559 **5.3. Revealing the variation in the urban structure based on multiplex**  
 560 **community detection**

561 We adopt the multiplex-Infomap algorithm to conduct community detection for  
 562 multimodal temporal and multiplex networks. Zones with similar interaction patterns  
 563 are grouped into a community and assigned a unique label, which is used to evaluate  
 564 the travel behavior of nodes/zones of multimodal transport modes over time or modes.  
 565 The variation or consistency of community labels directly indicates the variation of the  
 566 overall urban structure.

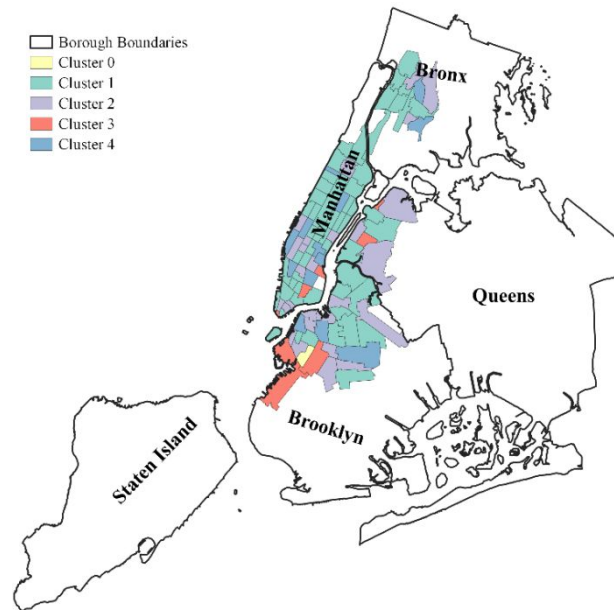
567 The first experiment is conducted on the multimodal network, a directed and  
 568 weighted zone-based interaction network of different modes in 2018 on three layers:  
 569 {Taxi2018, FHV2018, Bike2018}. This experiment examines whether newly emerged  
 570 shared transportation has zone-to-zone interactions similar to those of traditional taxis.  
 571 In total, 5 communities were identified in the multimodal network, and labels (0-4)  
 572 were given to the nodes on all layers.  
 573

	Taxi	FHV	Bike
Governor's Island/Ellis Island/Liberty Island	0	1	0
Yorkville East	1	1	1
Midtown Center	1	1	1
Clinton West	1	1	1
Times Sq/Theatre District	1	1	1
World Trade Center	1	1	1
Central Harlem North	1	1	1
Midtown North	1	1	1
Hudson Sq	1	1	1
Gramercy	1	1	1
Greenwich Village South	1	1	1
East Village	1	1	1
Red Hook	2	2	2
Downtown Brooklyn/MetroTech	2	2	2
Williamsburg (North Side)	2	2	2
Greenpoint	2	2	2
Boerum Hill	2	2	2
Sunnyside	3	3	3
Astoria Park	3	3	3
University Heights/Morris Heights	4	4	4
Claremont/Bathgate	4	4	4

0	Community 0
1	Community 1
2	Community 2
3	Community 3
4	Community 4

574  
 575  
 576  
 577  
 578  
 579  
 580

Figure 8. Community labels of zone across transport modes. Note that sample zones are displayed in this figure due to space limitations. There is actually 1 zone with varied community labels, 57 zones with all-1 community labels across modes, 27 zones with all-2 community labels, 8 zones with all-3 community labels, and 13 zones with all-4 community labels.



581  
582 Figure 9. Spatial distribution of the communities in the multimodal network  
583

584 A community detected in a mobility network indicates a set of nodes (i.e., zones)  
585 with similar interaction patterns. However, different from single-layer community  
586 detection, the obtained community labels in the multiplex network are comparable. For  
587 example, label 0 in the taxi layer and label 0 in the FHV layer indicate the same  
588 community role. Using this method, we are able to evaluate the similarity of the  
589 interaction behavior across transportation modes (i.e., layers). The community  
590 distribution of the multimodal network is shown in a matrix plot (Figure 8), where the  
591 Y axis represents zones (i.e., nodes) and X axis represent transport modes (i.e., taxi,  
592 FHV and bike layers). The spatial structure of the modal-network community is shown  
593 in Figure 9. The spatial clustering of cluster 1 is clearly observed in the central zones  
594 while clusters 2 and 3 are mostly located in distant areas.

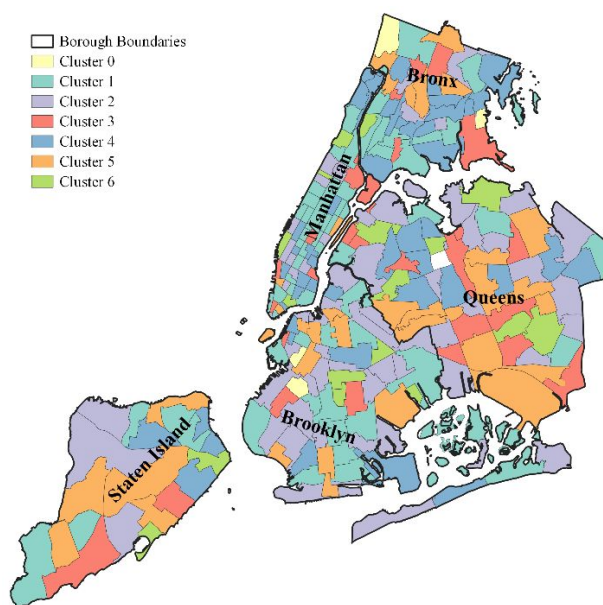
595 Sampled zones are visualized in Figure 8 due to limited space, and the actual  
596 number of different types of zones is illustrated in the title note. The zone type is  
597 identified according to the combinations of community labels across layers. In Figure  
598 8, the distribution of interaction behavior in different modes can be examined.  
599 Specifically, the three numbers in each horizontal line represent the community labels  
600 of a zone in each of the three layers (taxis, FHV's and bikes). If the three numbers are  
601 the same, it means the interaction patterns of the three transport modes are similar in  
602 this node (i.e., zone). Taking the second zone as an example, the community labels of  
603 the second zone (Yorkville East) are the same across different modes, which means that  
604 the interaction patterns among zones are similar regardless of whether taxis, FHV's, or  
605 bikes are chosen. In the first zone, *Governor's Island*, the community labels are {0, 1,  
606 0}. This means that the interaction behaviors are similar in terms of taking taxis and  
607 bikes while different interaction patterns are shown for FHV's. Interestingly, the  
608 community labels of most zones are consistent among taxis, FHV's, and bikes,  
609 excluding Gowanus (Figure 9). This indicates that the new transportation modes retain  
610 the same travel patterns as traditional taxis; specifically, the interaction patterns in such  
611 a multimodal network are the same.

	2013	2014	2015	2016	2017	2018
Rikers Island	1	3	1	7	3	0
Governor's Island/Ellis Island/Liberty Island	1	1	1	0	0	0
Great Kills Park	0	0	1	6	0	1
Little Italy/NoLiTa	1	1	1	1	1	1
JFK Airport	1	1	1	1	1	1
Hudson Sq	1	1	1	1	1	1
LaGuardia Airport	1	1	1	1	1	1
Freshkills Park	1	1	1	1	1	1
Ocean Parkway South	2	2	2	2	2	2
Prospect Heights	2	2	2	2	2	2
Bocrum Hill	2	2	2	2	2	2
Williamsburg (South Side)	2	2	2	2	2	2
Coney Island	2	2	2	2	2	2
Elmhurst/Maspeth	3	3	3	3	3	3
Flushing Meadows-Corona Park	3	3	3	3	3	3
North Corona	3	3	3	3	3	3
Maspeth	3	3	3	3	3	3
Westchester Village/Unionport	4	4	4	4	4	4
Soundview/Bruckner	4	4	4	4	4	4
West Farms/Bronx River	4	4	4	4	4	4
Kew Gardens Hills	5	5	5	5	5	5
Woodhaven	5	5	5	5	5	5
Bloomfield/Emerson Hill	6	6	6	6	6	6



612  
613  
614  
615  
616  
617  
618  
619  
620

Figure 10. Community labels of zones across years. Note that sample zones are displayed in this figure due to space limitations. There are actually 3 zones with varied community labels, 65 zones with all-1 community labels, 62 zones with all-2 community labels, 29 zones with all-3 community labels, 46 zones with all-4 community labels, 37 zones with all-5 community labels, and 18 zones with all-6 community labels.



621  
622  
623  
624  
625

Figure 11. Spatial distribution of the communities in the taxi temporal network

Multiplex community detection is also conducted in the temporal multiplex network of traditional taxis. This experiment investigates whether the interaction

626 patterns of traditional taxis vary from 2013 to 2018, the period when shared  
627 transportation was greatly expanding in the market. In Figure 10, we demonstrate the  
628 six communities identified across six years/layers, and the associated spatial structure  
629 is shown in Figure 11.

630 The community labels of traditional taxis are consistent across years in all zones  
631 except Country Club, Riverdale, Green-Wood Cemetery, and Gowanus. This result  
632 means that the interaction patterns of most zones remain stable in terms of traveling  
633 using traditional taxis. The result is similar to the findings in the first experiment on the  
634 multimodal network. That is, although there was dramatic variation in the market share  
635 among traditional taxis and shared transportation during these years, the interaction  
636 behavior at the zone level did not significantly change.

637

## 638 **6. Conclusion**

639 On-demand shared transportation (i.e., shared vehicles and shared bikes) has  
640 dramatically increased in recent years. In view of the advances in multilayer network  
641 analysis, this paper constructs empirical multiplex network models to explore how city  
642 zones are different from each other due to multidimensional urban flows. Specifically,  
643 this paper investigates travel patterns and associated urban structure in several ways.

644 Two centrality metrics, i.e., the multiplex degree and multiplex PageRank, are  
645 calculated in the multimodal network and temporal network. The centrality values  
646 attached to the spatial units reveal the hierarchical structure of location attractiveness.  
647 In a multimodal network, we found distinct differences between the uptown and  
648 downtown of Manhattan, which is also reported in the literature (Zhou et al., 2019).  
649 What is more interesting is the centrality spatial distribution in the temporal network  
650 across years, which shows that nearly the entirety of Manhattan and near-Manhattan  
651 zones all have the same high interaction flows. The possible reason is the differences  
652 in network layers defined in the multimodal network and temporal network. The results  
653 suggest that the selected layer significantly describes the dimension of variation, that  
654 is, the relatively large variation of the magnitude of the flow across transport modes  
655 while the relatively small variation of the flow across years. Both are valuable as the  
656 lens of multiframe urban structure while providing two different perspectives. The  
657 statistical distribution of network centrality is contrary previous studies that reported  
658 heavy-tailed human mobility patterns (Gonzalez et al., 2008; Liang et al., 2012; Zhao  
659 et al., 2015). In contrast, we observed a left skew of the degree and a slight right skew  
660 of PageRank. This pattern is particularly strong in the multimodal network (Figures 5a  
661 & 5b), which indicates that multimodal transit options make zones more connected to  
662 each other, resulting in a more balanced distribution of transit. Shared mobility may  
663 complement traditional taxis in distant areas but substitute in central areas (Kong et al.,  
664 2020).

665 Compared to the layer-by-layer analysis, the findings in community detection in  
666 multilayer analysis enable direct comparison in this study. Although the market share  
667 of traditional taxis has been greatly taken over by FHV and shared bikes, the identified  
668 interaction behavior shows that most zones are consistent across years and across  
669 modes. This suggests that shared transportation, a strong competitor as a travel mode,  
670 does not change collective travel behavior from zone to zone and may instead be  
671 affected by socioeconomic factors. For example, the interaction between a residential  
672 zone and a working zone remains the same regardless of the transport mode the traveler  
673 takes. The consistency of community patterns across transport modes in NYC agrees  
674 with another study using agent-based simulation (Lokhandwala & Cai, 2018). In this  
675 literature, they quantify the traffic conditions considering both traditional and shared

676 mobility services, suggesting that although shared mobility reduces traditional mode  
677 ridership, the overall service level remains the same. In this study, the consistency of a  
678 multimodal community can be understood as the stability of the overall interaction  
679 among places, although the ridership of each change.

680 Against initial expectation interaction variations of traditional taxis, community  
681 detection in taxi temporal networks shows consistent community labels across years.  
682 Although we select a period when shared mobility dramatically increases its market  
683 share, the stability of long-term interaction among places by taking taxis is observed in  
684 this study. A similar result is also reported in Riascos & Mateos (2020) using other  
685 network metrics. Our results may suggest that the long-term human mobility of taxis is  
686 generalizable in other cities, which may support the view that long-term taxi data are  
687 suitable for measuring the nature of human mobility. Another implication of a  
688 consistent community in a temporal network is that environmental factors may play a  
689 more influential role in changing taxi travel behavior rather than the emergence of  
690 shared mobility. As reported in Zhang et al. (2020), residential and commercial land  
691 uses have a significant impact on taxi ridership across many locations.

692 In this study, the relationship between the interaction pattern and land use was not  
693 systematically explored. However, we found some similar indications using network  
694 metrics. The results in Figure 7 provide similar indications that the factors of the urban  
695 context may determine the change in preferences for choosing modes instead of the  
696 emergence of shared transportation. In zones with 350 degrees, both taxis and FHV's  
697 grow in trip volume, although FHV's increase more rapidly. However, in 450-degree  
698 zones, the use of taxis decreases over time. The high degree zones indicate busy places  
699 such as Manhattan, and the drop in traditional taxis may be due to the feasibility and  
700 convenience of taking bikes or FHV's. These zones have a high network degree, which  
701 suggests that traffic jams may occur due to their high importance in a mobility network.  
702 In this context, shared bikes may even have greater roles in commuting. The results  
703 suggest rising travel demand and indicate that traditional taxis and shared vehicles do  
704 not have to be 'competitors' but can serve together to make distant transit more  
705 sufficient and diverse. We conclude that shared transportation influences travel choices  
706 in terms of ridership numbers due to its convenience in some areas, but it does not  
707 change the collective interaction patterns among zones compared to other modes.

708 There are some limitations of this work. Public transport flows are not considered  
709 when exploring the travel behavior and urban structure in this study. There are two  
710 major reasons. First, from our point of view, public transport is a fixed-route system  
711 that uses buses, metros, light rails, and other vehicles, which cannot reflect the on-  
712 demand mobility that uses mixed operating systems (e.g., offline and online). The on-  
713 demand mobility patterns would provide a special perspective to investigate the urban  
714 structure. Second, public transport data in the study area are currently unavailable. It  
715 would be great to use mixed datasets to explore the urban structure in future studies.  
716 However, our work will provide another empirical angle to understand urban dynamics.  
717 In addition, how these multiplex communities (e.g., urban structure) are associated with  
718 socioeconomic factors is also interesting but is out of the scope of this paper. The  
719 quantitative relation between these two is worthy of investigation in future studies.

## 720 **References**

721 Agryzkov, T., Tortosa, L., & Vicent, J. F. (2016). New highlights and a new centrality  
722 measure based on the Adapted PageRank Algorithm for urban networks. *Applied*  
723 *Mathematics and Computation*, 291, 14-29.

- 724 Aleta, A., Meloni, S., & Moreno, Y. (2017). A multilayer perspective for the analysis  
725 of urban transportation systems. *Scientific reports*, 7, 44359.
- 726 Alexander, L. P., & González, M. C. (2015). Assessing the impact of real-time  
727 ridesharing on urban traffic using mobile phone data. *Proc. UrbComp*, 1-9.
- 728 Barabási, A. L. (2005). Taming complexity. *Nature physics*, 1(2), 68-70.
- 729 Barthélemy, M. (2011). Spatial networks. *Physics Reports*, 499(1-3), 1-101.
- 730 Battiston, F., Nicosia, V., & Latora, V. (2017). The new challenges of multiplex  
731 networks: Measures and models. *The European Physical Journal Special Topics*,  
732 226(3), 401-416.
- 733 Batty, M. (2013). *The new science of cities*. MIT press.
- 734 Campbell, K. B., & Brakewood, C. (2017). Sharing riders: How bikesharing impacts  
735 bus ridership in New York City. *Transportation Research Part A: Policy and  
736 Practice*, 100, 264-282.
- 737 Cannon, S., & Summers, L. H. (2014). How Uber and the sharing economy can win  
738 over regulators. *Harvard business review*, 13(10), 24-28.
- 739 Cao, M., Ma, S., Huang, M., Lü, G., & Chen, M. (2019). Effects of free-floating shared  
740 bicycles on urban public transportation. *ISPRS International Journal of Geo-  
741 Information*, 8(8), 323.
- 742 Cardillo, A., Zanin, M., Gómez-Gardenes, J., Romance, M., del Amo, A. J. G., &  
743 Boccaletti, S. (2013). Modeling the multi-layer nature of the European Air  
744 Transport Network: Resilience and passengers re-scheduling under random  
745 failures. *The European Physical Journal Special Topics*, 215(1), 23-33.
- 746 Chen, B. Y., Yuan, H., Li, Q., Shaw, S. L., Lam, W. H., & Chen, X. (2016).  
747 Spatiotemporal data model for network time geographic analysis in the era of big  
748 data. *International Journal of Geographical Information Science*, 30(6), 1041-  
749 1071.
- 750 De Domenico, M., Porter, M. A., & Arenas, A. (2015a). MuxViz: a tool for multilayer  
751 analysis and visualization of networks. *Journal of Complex Networks*, 3(2), 159-  
752 176.
- 753 De Domenico, M., Solé-Ribalta, A., Cozzo, E., Kivelä, M., Moreno, Y., Porter, M. A.,  
754 Gómez, S. & Arenas, A. (2013). Mathematical formulation of multilayer  
755 networks. *Physical Review X*, 3(4), 041022.
- 756 De Domenico, M., Solé-Ribalta, A., Omodei, E., Gómez, S., & Arenas, A. (2015b).  
757 Ranking in interconnected multilayer networks reveals versatile nodes. *Nature  
758 communications*, 6(1), 1-6.
- 759 Dimitrov, S. D., & Ceder, A. A. (2016). A method of examining the structure and  
760 topological properties of public-transport networks. *Physica A: Statistical  
761 Mechanics and its Applications*, 451, 373-387.
- 762 Ding, R., Ujang, N., bin Hamid, H., Manan, M. S. A., He, Y., Li, R., & Wu, J. (2018).  
763 Detecting the urban traffic network structure dynamics through the growth and  
764 analysis of multi-layer networks. *Physica A: Statistical Mechanics and its  
765 Applications*, 503, 800-817.
- 766 Ding, Y., Yan, E., Frazho, A., & Caverlee, J. (2009). PageRank for ranking authors in  
767 co-citation networks. *Journal of the American Society for Information Science  
768 and Technology*, 60(11), 2229-2243.
- 769 Faghih-Imani, A., Anowar, S., Miller, E. J., & Eluru, N. (2017). Hail a cab or ride a  
770 bike? A travel time comparison of taxi and bicycle-sharing systems in New York  
771 City. *Transportation Research Part A: Policy and Practice*, 101, 11-21.
- 772 Ferber, C., Holovatch, Y., & Palchykov, V. (2005). Scaling in public transport networks.  
773 *Condens Matter Phys.* 8(141):225-234.

- 774 Gao, X., & Tian, L. (2019). Effects of awareness and policy on green behavior  
775 spreading in multiplex networks. *Physica A: Statistical Mechanics and its*  
776 *Applications*, 514, 226-234.
- 777 Gonzalez, M. C., Hidalgo, C. A., & Barabasi, A. L. (2008). Understanding individual  
778 human mobility patterns. *nature*, 453(7196), 779-782.
- 779 Grünwald, P. D., & Grunwald, A. (2007). *The minimum description length principle*.  
780 MIT press.
- 781 Halu, A., Mondragón, R. J., Panzarasa, P., & Bianconi, G. (2013). Multiplex  
782 pagerank. *PloS one*, 8(10).
- 783 Halu, A., Mukherjee, S. and Bianconi, G., 2014. Emergence of overlap in ensembles of  
784 spatial multiplexes and statistical mechanics of spatial interacting network  
785 ensembles. *Physical Review E*, 89(1), p.012806.
- 786 Handy, S. (1996). Methodologies for exploring the link between urban form and travel  
787 behavior. *Transportation Research Part D: Transport and Environment*, 1(2), 151-165.
- 788 Hochmair, H. H. (2016). Spatiotemporal pattern analysis of taxi trips in New York  
789 City. *Transportation research record*, 2542(1), 45-56.
- 790 Hristova, D., Musolesi, M., & Mascolo, C. (2014, May). Keep your friends close and  
791 your facebook friends closer: A multiplex network approach to the analysis of  
792 offline and online social ties. In *Eighth International AAAI Conference on*  
793 *Weblogs and Social Media*.
- 794 Jia, C., Du, Y., Wang, S., Bai, T., & Fei, T. (2019). Measuring the vibrancy of urban  
795 neighborhoods using mobile phone data with an improved PageRank  
796 algorithm. *Transactions in GIS*, 23(2), 241-258.
- 797 Jiang, B., & Yao, X. (Eds.). (2010). Geospatial analysis and modelling of urban  
798 structure and dynamics (Vol. 99). *Springer Science & Business Media*.
- 799 Kivelä, M., Arenas, A., Barthelemy, M., Gleeson, J. P., Moreno, Y., & Porter, M. A.  
800 (2014). Multilayer networks. *Journal of complex networks*, 2(3), 203-271.
- 801 Klinger, T., & Lanzendorf, M. (2016). Moving between mobility cultures: what affects  
802 the travel behavior of new residents?. *Transportation*, 43(2), 243-271.
- 803 Kong, H., Zhang, X., & Zhao, J. (2020). How does ridesourcing substitute for public  
804 transit? A geospatial perspective in Chengdu, China. *Journal of Transport*  
805 *Geography*, 86, 102769.
- 806 Li, Y., Yang, L., Shen, H., & Wu, Z. (2019). Modeling intra-destination travel behavior  
807 of tourists through spatio-temporal analysis. *Journal of destination marketing &*  
808 *management*, 11, 260-269.
- 809 Li, Z., Hong, Y., & Zhang, Z. (2016, September). An empirical analysis of on-demand  
810 ride sharing and traffic congestion. In *Proc. International Conference on*  
811 *Information Systems*.
- 812 Liang, X., Zheng, X., Lv, W., Zhu, T., & Xu, K. (2012). The scaling of human mobility  
813 by taxis is exponential. *Physica A: Statistical Mechanics and its*  
814 *Applications*, 391(5), 2135-2144.
- 815 Liu, X., Gong, L., Gong, Y., & Liu, Y. (2015). Revealing travel patterns and city  
816 structure with taxi trip data. *Journal of Transport Geography*, 43, 78-90.
- 817 Lokhandwala, M., & Cai, H. (2018). Dynamic ride sharing using traditional taxis and  
818 shared autonomous taxis: A case study of NYC. *Transportation Research Part*  
819 *C: Emerging Technologies*, 97, 45-60.
- 820 Luo, X., Dong, L., Dou, Y., Zhang, N., Ren, J., Li, Y., Sun, L. & Yao, S. (2017).  
821 Analysis on spatial-temporal features of taxis' emissions from big data informed  
822 travel patterns: a case of Shanghai, China. *Journal of cleaner production*, 142,  
823 926-935.

- 824 Mucha, P. J., & Porter, M. A. (2010). Communities in multislice voting  
825 networks. *Chaos: An Interdisciplinary Journal of Nonlinear Science*, 20(4),  
826 041108
- 827 Newman, M. E. (2006). Modularity and community structure in networks. *Proceedings*  
828 *of the national academy of sciences*, 103(23), 8577-8582.
- 829 Newman, M. E., & Girvan, M. (2004). Finding and evaluating community structure in  
830 networks. *Physical review E*, 69(2), 026113.
- 831 Nicosia, V., Bianconi, G., Latora, V., & Barthelemy, M. (2013). Growing multiplex  
832 networks. *Physical review letters*, 111(5), 058701.
- 833 Page, L., Brin, S., Motwani, R., & Winograd, T. (1999). *The PageRank citation ranking:*  
834 *Bringing order to the web*. Stanford InfoLab.
- 835 Parshani, R., Rozenblat, C., Ietri, D., Ducruet, C., & Havlin, S. (2011). Inter-similarity  
836 between coupled networks. *EPL (Europhysics Letters)*, 92(6), 68002.
- 837 Paulssen, M., Temme, D., Vij, A., & Walker, J. L. (2014). Values, attitudes and travel  
838 behavior: a hierarchical latent variable mixed logit model of travel mode  
839 choice. *Transportation*, 41(4), 873-888.
- 840 Qian, X., Zhan, X., & Ukkusuri, S. V. (2015). Characterizing urban dynamics using  
841 large scale taxicab data. In *Engineering and Applied Sciences Optimization* (pp.  
842 17-32). Springer, Cham.
- 843 Ratti, C., Sobolevsky, S., Calabrese, F., Andris, C., Reades, J., Martino, M., Claxton,  
844 R. & Strogatz, S. H. (2010). Redrawing the map of Great Britain from a network  
845 of human interactions. *PloS one*, 5(12), e14248.
- 846 Riascos, A. P., & Mateos, J. L. (2020). Networks and long-range mobility in cities: A  
847 study of more than one billion taxi trips in New York City. *Scientific*  
848 *reports*, 10(1), 1-14.
- 849 Rodrigue, J. P. (2020). The geography of transport systems. *Routledge*.
- 850 Sarkar, S., Chawla, S., Ahmad, S., Srivastava, J., Hammady, H., Filali, F., Znaidi, W.  
851 & Borge-Holthoefer, J. (2017). Effective urban structure inference from traffic  
852 flow dynamics. *IEEE Transactions on Big Data*, 3(2), 181-193.
- 853 Shen, J., Liu, X., & Chen, M. (2017). Discovering spatial and temporal patterns from  
854 taxi-based Floating Car Data: A case study from Nanjing. *GIScience & Remote*  
855 *Sensing*, 54(5), 617-638.
- 856 Shmueli, E., Mazeh, I., Radaelli, L., Pentland, A. S., & Altshuler, Y. (2015, March).  
857 Ride sharing: a network perspective. In *International Conference on Social*  
858 *Computing, Behavioral-Cultural Modeling, and Prediction* (pp. 434-439).  
859 Springer, Cham.
- 860 Strano, E., Shai, S., Dobson, S., & Barthelemy, M. (2015). Multiplex networks in  
861 metropolitan areas: generic features and local effects. *Journal of The Royal*  
862 *Society Interface*, 12(111), 20150651.
- 863 Tao, S., Rohde, D., & Corcoran, J. (2014). Examining the spatial-temporal dynamics  
864 of bus passenger travel behaviour using smart card data and the flow-  
865 comap. *Journal of Transport Geography*, 41, 21-36.
- 866 Wallsten, S. (2015). The competitive effects of the sharing economy: how is Uber  
867 changing taxis. *Technology Policy Institute*, 22, 1-21.
- 868 Wen, T. H. (2015). Geographically modified PageRank algorithms: Identifying the  
869 spatial concentration of human movement in a geospatial network. *PloS*  
870 *one*, 10(10), e0139509.
- 871 Xu, J., Li, A., Li, D., Liu, Y., Du, Y., Pei, T., Ma, T. & Zhou, C. (2017). Difference of  
872 urban development in China from the perspective of passenger transport around  
873 Spring Festival. *Applied Geography*, 87, 85-96.

- 874 Xu, Y., Chen, D., Zhang, X., Tu, W., Chen, Y., Shen, Y., & Ratti, C. (2019). Unravel  
875 the landscape and pulses of cycling activities from a dockless bike-sharing  
876 system. *Computers, Environment and Urban Systems*, 75, 184-203.
- 877 Yang, Y., Heppenstall, A., Turner, A., & Comber, A. (2019). A spatiotemporal and  
878 graph-based analysis of dockless bike sharing patterns to understand urban flows  
879 over the last mile. *Computers, Environment and Urban Systems*, 77, 101361.
- 880 Yildirimoglu, M., & Kim, J. (2018). Identification of communities in urban mobility  
881 networks using multi-layer graphs of network traffic. *Transportation Research*  
882 *Part C: Emerging Technologies*, 89, 254-267.
- 883 Yu, X., Lilburn, T. G., Cai, H., Gu, J., Korkmaz, T., & Wang, Y. (2017). PageRank  
884 influence analysis of protein-protein association networks in the malaria parasite  
885 *Plasmodium falciparum*. *International Journal of Computational Biology and*  
886 *Drug Design*, 10(2), 137-156.
- 887 Zhang, X., Huang, B., & Zhu, S. (2020). Spatiotemporal Varying Effects of Built  
888 Environment on Taxi and Ride-Hailing Ridership in New York City. *ISPRS*  
889 *International Journal of Geo-Information*, 9(8), 475.
- 890 Zhang, X., Xu, Y., Tu, W., & Ratti, C. (2018). Do different datasets tell the same story  
891 about urban mobility—A comparative study of public transit and taxi  
892 usage. *Journal of Transport Geography*, 70, 78-90.
- 893 Zhao, D., Li, L., Peng, H., Luo, Q., & Yang, Y. (2014). Multiple routes transmitted  
894 epidemics on multiplex networks. *Physics Letters A*, 378(10), 770-776.
- 895 Zhao, K., Musolesi, M., Hui, P., Rao, W., & Tarkoma, S. (2015). Explaining the power-  
896 law distribution of human mobility through transportation modality  
897 decomposition. *Scientific reports*, 5(1), 1-7.
- 898 Zhong, C., Arisona, S. M., Huang, X., Batty, M., & Schmitt, G. (2014). Detecting the  
899 dynamics of urban structure through spatial network analysis. *International*  
900 *Journal of Geographical Information Science*, 28(11), 2178-2199.
- 901 Zhou, J., & Qiu, G. (2018). China's high-speed rail network construction and planning  
902 over time: a network analysis. *Journal of Transport Geography*, 70, 40-54.
- 903 Zhou, Y., Chen, H., Wu, Y., Wu, J., Li, J., & Chen, L. (2019, February). A Method for  
904 Analyzing Pick-Up/Drop-Off Distribution of Taxi Passengers' in Urban Areas  
905 Based on Dynamical Network View. In *2019 IEEE International Conference on*  
906 *Big Data and Smart Computing (BigComp)* (pp. 1-8). IEEE.